JVI Journals.ASM.org

Critical Role for Voltage-Dependent Anion Channel 2 in Infectious Bursal Disease Virus-Induced Apoptosis in Host Cells via Interaction with VP5

Zhonghua Li, Yongqiang Wang, Yanfei Xue, Xiaoqi Li, Hong Cao, and Shijun J. Zheng

State Key Laboratory of Agrobiotechnology, Key Laboratory of Animal Epidemiology and Zoonosis, Ministry of Agriculture, and College of Veterinary Medicine, China Agricultural University, Beijing, China

Infectious bursal disease (IBD) is an acute, highly contagious, and immunosuppressive avian disease caused by IBD virus (IBDV). Although IBDV-induced host cell apoptosis has been established, the underlying molecular mechanism is still unclear. We report here that IBDV viral protein 5 (VP5) is a major apoptosis inducer in DF-1 cells by interacting with the voltage-dependent anion channel 2 (VDAC2) in the mitochondrion. We found that in DF-1 cells, VP5-induced apoptosis can be completely abolished by 4,4′-diisothiocyanatostibene-2,2′-disulfonic acid (DIDS), an inhibitor of VDAC. Furthermore, knockdown of VDAC2 by small interfering RNA markedly inhibits IBDV-induced apoptosis associated with decreased caspase-9 and -3 activation and cytochrome *c* release, leading to increased IBDV growth in host cells. Thus, VP5-induced apoptosis during IBDV infection is mediated by interacting with VDAC2, a protein that appears to restrict viral replication via induction of cell death.

Infectious bursal disease (IBD), also called Gumboro disease, is an acute, highly contagious disease in young chickens that occurs across the world (22). Its causative agent, infectious bursal disease virus (IBDV), destroys its target cells, the B-lymphocyte precursors (16, 28, 41). IBDV infection may cause mortality in naïve chickens and very high mortality in chickens with low levels of neutralizing antibodies or no mortality at all but a high degree of immunosuppression (20). The diseased chickens suffer from a severe immunosuppression which leads to an increased susceptibility to other pathogens (31).

IBDV is an *Avibirnavirus* belonging to the *Birnaviridae* family, which is composed of nonenveloped viruses containing two segments of double-stranded RNA (segments A and B) (1). Whereas the short RNA, segment B (2.8 kb), encodes VP1, an RNA-dependent RNA polymerase (RdRp) (19, 36), segment A, the large molecule (3.17 kb), contains two partially overlapping open reading frames (ORFs) (12, 30, 31). The first ORF encodes the nonstructural viral protein 5 (VP5), and the second one encodes a 110-kDa polyprotein precursor that can be cleaved by the proteolytic activity of VP4 to form viral proteins VP2, VP3, and VP4 (1, 9, 10, 12). VP2 and VP3 are the major structural proteins, constituting 51% and 40% of the virion, respectively (5). VP4 is a classical *cis*-cleavage protein, and its *trans* activity is present but acts later in the life cycle of a double-stranded RNA virus (2, 14). VP4 is able to cleave in *trans* and is responsible for the interdomain proteolytic autoprocessing of the pVP2-VP4-VP3 polyprotein encoded by RNA segment A into the pVP2 precursor (48 kDa), as well as VP4 (28 kDa) and VP3 (32 kDa) (2, 31). VP5, a highly basic, cysteine-rich, 17-kDa nonstructural (NS) protein, is conserved among all serotype I isolates of IBDV strains. This protein is not present in the virion and can be detected only in IBDV-infected cells (21). Ectopic expression of VP5 in chicken embryo fibroblasts (CEFs), BSC-1, or Cos-1 cells revealed that this protein accumulates within the plasma membrane and induces cell lysis (18). An IBDV mutant lacking VP5 expression exhibited decreased apoptotic effects in cell culture, suggesting that this protein plays a role in the induction of apoptosis during IBDV infection (40, 41).

Although VP5 is known to induce apoptosis, the exact molecular mechanism underlying such induction remains elusive. In this study, we found that VP5 interacts with the voltage-dependent anion channel 2 (VDAC2) in the mitochondrion of host cells. In support of a role of VDAC2 in cell death induced by VP5, inhibition of its activity with 4,4′-diisothiocyanatostibene-2,2′-disulfonic acid (DIDS) led to a complete abolishment of apoptosis in the presence of viral protein. Furthermore, knockdown of VDAC2 by small interfering RNA (siRNA) markedly inhibited IBDV-induced apoptosis, accompanied by increased IBDV replication.

MATERIALS AND METHODS

Cells and virus. Both DF-1 (immortal chicken embryo fibroblast) and HEK293T cells were obtained from ATCC. All cells were cultured in Dulbecco modified Eagle medium (DMEM; Invitrogen) supplemented with 10% fetal bovine serum (FBS) in a 5% CO_2 incubator. *Lx*, a cell culture-adapted IBDV strain, was kindly provided by Jue Liu (Beijing Academy of Agriculture and Forestry, Beijing, China).

Reagents. All the restriction enzymes were purchased from NEB. pCMV-Myc, pRK5-FLAG, pDsRed-monomer-N1, and pEGFP-C1 vectors were obtained from Clontech. Annexin V-fluorescein isothiocyanate (FITC), DIDS, propidium iodide (PI), and anti-FLAG (F1804) antibody were purchased from Sigma. Anti-c-Myc (sc-40), anti-green fluorescent protein (anti-GFP; sc-9996), and anti-β-actin (sc-1616-R) monoclonal antibodies were obtained from Santa Cruz Biotechnology. Rabbit anti-VDAC2 polyclonal antibodies (ab47104) were purchased from Abcam (United Kingdom). Anti-cytochrome *c* mouse monoclonal antibody

Received 23 August 2011 Accepted 11 November 2011
Published ahead of print 23 November 2011
Address correspondence to Shijun J. Zheng, sjzheng@cau.edu.cn.
Z. Li and Y. Wang contributed equally to this article.

doi:10.1128/JVI.06104-11

(AP1029) was purchased from Merck (Germany). Caspase-3 and -9 activity assay kits were obtained from BioVision.

Construction of plasmids. IBDV VP1, VP2, VP3, VP4, and VP5 were cloned from IBDV strain *Lx* using the following specific primers: for VP1, sense primer 5′-ATGAGTGACGTTTCAATAGTCC-3′ and antisense primer 5′-CTATTGGCGGCTCTCTTTCTG-3′ (GenBank accession number 219564808); for VP2, sense primer 5′-ATGACGAACCTGCAAG ATCAAA-3′ and antisense primer 5′-CCTTAGGGCCCGGATTATGTC TT-3′ (GenBank accession number 171906501); for VP3, sense primer 5′-CGTTTCCCTCACAATCCACGCGA-3′ and antisense primer 5′-CT CAAGGTCCTCATCAGAGACGGT-3′ (GenBank accession number 126032566); for VP4, sense primer 5′-AGGATAGCTGTGCCGGTGGTC TCCACAT-3′ and antisense primer 5′-TTTGATGAACGTTGCCCAGT T-3′ (GenBank accession number 6539893); and for VP5, sense primer 5′-ATGGTTAGTAGAGATCAGA-3′ and antisense primer 5′-TCACTC AGGCTTCCTTGGAAGGT-3′ (GenBank accession number 24306007). VDAC2 was cloned from cDNA of DF-1 cells using specific primers (sense primer 5′-ATGGCGATTCCTCCATCATAT-3′ and antisense primer 5′-TTAGGCCTCCAATTCCAGG-3′ [GenBank accession number 395498]). pCMV-Myc-VDAC2, pDsRed-VP5, pEGFP-VDAC2, pEGFP-VP2, pEGFP-VP3, pEGFP-VP4, pEGFP-VP5, pRK-FLAG-VP5, and truncated pCMV-Myc-VP5 expression plasmids (Δ1, amino acids [aa] 50 to 145; Δ2, aa 100 to 145; Δ3, aa 1 to 100; Δ4, aa 1 to 50) were constructed by standard molecular biology techniques. All the primers were synthesized by Augct Company (Beijing, China).

Apoptosis assay. DF-1 cells (6.0×10^5) were seeded on six-well plates and cultured overnight. Cells were transfected with pEGFP-C1, pEGFP-VP2, pEGFP-VP3, pEGFP-VP4, or pEGFP-VP5 plasmids by Lipofectamine LTX. Twenty-four hours after transfection, cells were trypsinized and stained by PI (1 μg/ml) for 10 min at room temperature. Suspended cells were then analyzed by flow cytometry. GFP-positive cells were gated for apoptosis analysis. Fluorescence-activated cells sorter data were analyzed with CellQuest software (BD).

Mock-infected or IBDV-infected DF-1 cells were harvested and washed twice with phosphate-buffered saline (PBS), resuspended in a buffer (135 mM NaCl, 10 mM HEPES, 5 mM $CaCl_2$), and incubated with FITC-conjugated annexin V and PI (1 μg/ml) for 15 min at room temperature. Samples were subjected to flow cytometry analysis as described above.

Coimmunoprecipitation and Western blot analysis. For immunoprecipitation, HEK293T cells or DF-1 cells (6×10^5) were seeded on six-well plates and cultured for 24 h before cotransfected with pCMV-Myc-VDAC2 and pRK5-FLAG-VP5 or empty vectors as controls by the standard calcium phosphate precipitation. Twenty-four hours after transfection, cell lysates were prepared using a nondenaturing lysis buffer (50 mM Tris-HCl, pH 8.0, 150 mM NaCl, 1% NP-40, 5 mM EDTA, 10% glycerol, 10 mM dithiothreitol, 1× complete cocktail protease inhibitor). The cell lysates were incubated with 2 μg of anti-FLAG antibody at 4°C for 2 h and then mixed with 20 μl of a 50% slurry of protein A/G plus agarose and incubated for another 2 h. Beads were washed three times with the lysis buffer and boiled with 2× SDS loading buffer for 10 min. The samples were fractionated by electrophoresis on 12% SDS-polyacrylamide gels, and resolved proteins were transferred onto polyvinylidene difluoride membranes. After blocking with 5% skim milk, the membranes were incubated with either anti-Myc or anti-FLAG antibodies, followed by an appropriate horseradish peroxidase-conjugated secondary antibody. Blots were developed using an enhanced chemiluminescence (ECL) kit. For endogenous VDAC2 pulldown assay, HEK293T or DF-1 cells were transfected with pRK5-FLAG-VP5 or with empty vector. Thirty-six hours after transfection, the cell lysates were subjected to immunoprecipitation with anti-FLAG antibody and immunoblotted with anti-VDAC2 or anti-FLAG antibodies.

Confocal laser scanning microscopy assays. HEK293T cells (2×10^5) were seeded on coverslips in 24-well plates and were cultured overnight before transfection with pEGFP-C1-VDAC2 and pDsRed-N1-VP5. Twenty-four hours after transfection, the cells were fixed with 1% paraformaldehyde and the nuclei were stained with 4′,6-diamidino-2-phenylindole (DAPI). For endogenous protein staining, the fixed cells were permeabilized with 0.1% Triton X-100 for 15 min, blocked with 1% bovine serum albumin, and then probed with the anti-VDAC2 antibody at room temperature for 1 h. After three washes with PBS, the cells were incubated with rhodamine (tetramethyl rhodamine isocyanate [TRITC])-conjugated goat antirabbit antibody. After three washes with PBS, the cells were stained for nuclei with DAPI. For subcellular organelle staining, the transfected cells were incubated with the MitoTracker probe in 5% CO_2 at 37°C for 30 min. The samples were analyzed with a laser confocal scanning microscope (Nikon C1 standard detector; Japan).

Immunofluorescence antibody assay (IFA). HEK293T cells were infected with IBDV at a multiplicity of infection (MOI) of 10 and incubated for 3 h at 37°C. Uninfected HEK293T cells were used as negative controls. Three hours after incubation, the medium was changed for fresh DMEM with 2% FBS and further incubated for 24 h. After incubation, the cells were fixed with 4% paraformaldehyde, permeabilized with 0.2% Triton X-100, blocked with 1% bovine serum albumin, and incubated with mouse anti-VP5 antiserum and rabbit anti-VDAC2 antibodies, followed by FITC-conjugated goat antimouse antibody (green) and TRITC-conjugated goat antirabbit antibody (red). Nuclei were counterstained with DAPI (blue). The cell samples were observed with a laser confocal scanning microscope.

RNA interference (RNAi) knockdown of VDAC2. siRNAs designed by the Genechem Company (Shanghai, China) were used to knock down VDAC2 in DF-1 cells. The sequences of siRNA for targeting VDAC2 in DF-1 cells included RNAi#1 (sense, 5′-GCUUGGAGACCAAAUACAAT T-3′; antisense, 5′-UUGUAUUUGGUCUCCAAGCTT-3′), RNAi#2 (sense, 5′-GACUGGAGACUUCCAGCUUTT-3′; antisense, 5′-AAGCU GGAAGUCUCCAGUCTT-3′), RNAi#3 (sense, 5′-GCUUCACACCAAU GUCAAUTT-3′; antisense, 5′-AUUGACAUUGGUGUGAAGCTT-3′), and negative siRNA control (sense, 5′-UUCUCCGAACGUGUCACGUT T-3′; antisense, 5′-ACGUGACACGUUCGGAGAATT-3′). To transfect cells with the interference RNAs against VDAC2, we seeded DF-1 cells (4×10^5) cells on six-well plates and cultured the cells for at least 20 h prior to transfection. The cells were transfected with siRNA using RNAiMAX reagent, according to the manufacturer's instructions (Invitrogen). Double transfections were performed at a 24-h interval. Forty-eight hours after the second transfection, cells were harvested for further analysis.

Caspase-3 and -9 activity assays. DF-1 cells (4×10^5) were seeded on six-well plates and were mock infected or infected with IBDV at an MOI of 10. Infected cells were incubated for 20 h before being trypsinized. Lifted cells were washed with cold PBS, resuspended in 50 μl of chilled cell lysis buffer, and incubated on ice for 15 min. The cell lysates were centrifuged at 10,000 × *g* for 15 min. The supernatants were collected and frozen at −70°C. Caspase-3 and -9 activities of samples were measured with a fluorescence plate reader (spectra Max M5; MD) using fluorescent substrate DEVD-AFC (synthetic caspase-3 substrate) or LEHD-AFC (synthetic caspase-9 substrate), according to the manufacturer's instructions. Results of all experiments were reported as means ± standard deviations (SDs).

Preparation of cytosolic fractions for measurement of cytochrome *c* release. The isolation of mitochondria and cytosol was performed using a cell mitochondrion isolation kit (Beyotime Institute of Biotechnology, China). Briefly, untreated cells or cells receiving VDAC2-specific siRNAs or control siRNA were incubated in 100 μl in ice-cold mitochondrion lysis buffer on ice for 10 min. Cell suspensions were then homogenized on ice with Dounce grinders. The homogenates were centrifuged at 800 × *g* for 10 min, and the supernatant was collected and centrifuged again at 12,000 × *g* for 30 min. The supernatant was collected and stored at −80°C before the examination of cytochrome *c* release by Western blotting.

Measurement of IBDV growth in DF-1 cells. Untreated cells or cells receiving VDAC2-specific siRNAs or control siRNA were infected with IBDV at an MOI of 10, and cell cultures were collected at different time

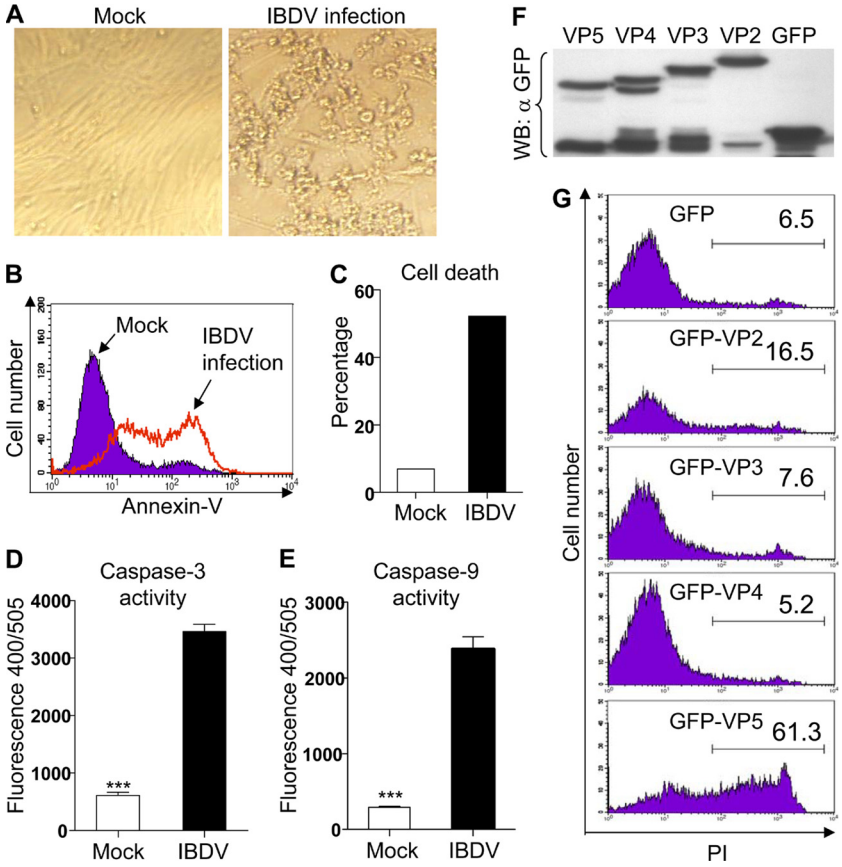

FIG 1 Induction of DF-1 cell death by the viral components of IBDV. (A) IBDV infection caused a CPE in DF-1 cells. DF-1 cells were mock infected or infected with IBDV at an MOI of 10. Forty-eight hours postinfection, cells were observed by phase-contrast microscopy. (B) Flow cytometry analysis of IBDV-induced cell death in DF-1 cells. Thirty-six hours postinfection, cells were harvested and stained with annexin V-FITC and analyzed by flow cytometry. Mock-infected cells were used as controls. (C) Determination of cell death in IBDV-infected DF-1 cells by trypan blue dye exclusion assay. DF-1 cells were infected as described for panel A. Forty-eight hours postinfection, dead cells were counted under a microscope after trypan blue dye staining. Data are representative of three independent experiments. (D and E) Activities of caspase-3 (D) and caspase-9 (E) in DF-1 cells after IBDV infection. DF-1 cells were infected as described for panel A. Twenty hours after infection, the enzymatic activities of caspase-3 and caspase-9 were examined as described in Materials and Methods. Graphs show means ± SD ($n = 3$). ***, $P < 0.001$. (F) Expression of GFP-VP2, -VP3, -VP4, or -VP5 fusion proteins in DF-1 cells. DF-1 cells (6×10^5) were seeded on six-well plates and cultured overnight. Cells were transfected with pEGFP-C1, pEGFP-VP2, pEGFP-VP3, pEGFP-VP4, or pEGFP-VP5 plasmid. Twenty-four hours after transfection, cell lysates were prepared and examined with Western blotting (WB) using anti-GFP antibodies. (G) Flow cytometry analysis of apoptosis in DF-1 cells transfected to express GFP, GFP-VP2, GFP-VP3, GFP-VP4, or GFP-VP5 fusion proteins. DF-1 cells were transfected with different plasmids as described for panel F. Twenty-four hours after transfection, cells were harvested, stained with PI, and analyzed by flow cytometry. GFP-positive cells were gated for further analysis of PI staining-positive cells. Data are representative of three independent experiments.

points (12, 24, 48, 72 h) after infection. The culture samples were freeze-thawed three times and centrifuged at 2,000 × *g* for 10 min. The viral contents in the supernatants were titrated using 50% tissue culture infective doses ($TCID_{50}$) in DF-1 cells. Briefly, the viral solution was diluted by 10-fold in DMEM. A 100-μl aliquot of each diluted sample was added to the wells of 96-well plates, followed by addition of 100 μl of DF-1 cells at a density of 5×10^5 cells/ml. Cells were cultured for 5 days at 37°C in 5% CO_2. Tissue culture wells with a cytopathic effect (CPE) were determined to be positive. The titer was calculated on the basis of a previously described method (24).

Statistical analysis. The significance of the differences between IBDV-infected cells and controls in caspase-9 and -3 activities, between VDAC2 RNAi cells and controls in caspase-9 and -3 activities and in viral growth, and between DIDS-treated cells and controls in viral growth was determined by the Mann-Whitney test or analysis of variance (ANOVA) accordingly.

RESULTS

The VP5 protein is mainly responsible for IBDV-induced apoptosis in DF-1 cells. IBDV is capable of replicating in multiple types of cells, including chicken B cells (25), CEF and DF-1 cells (37), and Vero and HEK293T cells (33). To determine if IBDV induces a CPE in DF-1 cells, we infected cells of this cell line with the *Lx* strain of this virus at an MOI of 10. A typical CPE was observed 48 h after infection (Fig. 1A). To further analyze the cell biological features associated with an IBDV-induced CPE in DF-1 cells, samples stained for annexin V were analyzed by flow cytometry. As shown in Fig. 1B, the number of annexin V-positive cells markedly increased after IBDV infection compared to that of mock-infected cells. In addition, at 48 h after IBDV infection, cells succumbed to death at a rate 7.5 times of that for cells with mock infection, as examined by trypan blue dye exclusion assay (Fig. 1C). Consistent with these data, the activities of caspase-3 and -9 of IBDV-infected samples were significantly greater than those of controls ($P < 0.001$) (Fig. 1D and E). These data indicate that IBDV infection causes apoptosis in DF-1 cells with involvement of caspase-3 and -9 activation.

Since IBDV infection caused apoptosis in DF-1 cells, we pro-

posed that one or more components of IBDV trigger host cell death by engaging host proteins involved in regulating this cellular process. To test this hypothesis, we cloned the *vp1*, *vp2*, *vp3*, *vp4*, and *vp5* genes from the IBDV *Lx* strain. As *vp1* is known to encode an RNA-dependent RNA polymerase (RdRp) (19, 36), we primarily focused on the cell-death-induction ability of VP2, VP3, VP4, and VP5. We made a GFP fusion for each of these proteins and expressed them in DF-1 cells by transfection. All four protein fusions were expressed well in this cell line (Fig. 1F). Importantly, we found that both VP2 and VP5 could cause apoptosis in DF-1 cells but VP5 exhibited a much higher potency in the induction of the phenotype (Fig. 1G). In contrast, VP3 and VP4 had little apoptosis-inducing activity. Taken together, these data suggest that VP5 is the major viral component responsible for IBDV-induced apoptosis in DF-1 cells.

VP5 interacts with VDAC2. After the identification of VP5 as the major viral protein responsible for inducing cell death in DF-1 cells, we furthered our investigation to study the mechanism of such induction by searching for its cellular targets. To this end, we used VP2 to VP5 as bait in the yeast two-hybrid system to screen a cDNA library generated from the chicken bursa of Fabricius. Among the positive clones, VDAC2 showed up with a higher frequency (data not shown). Among the proteins that potentially interact with VP5, VDAC2 proteins were identified 5 times. VDAC2 might be relevant to VP5 function because it is one of the VDAC isoforms involved in apoptosis by regulating the permeability of the outer mitochondrial membrane via its pore-forming activity (3, 4, 29, 42). Thus, we constructed a plasmid that allows the expression of Myc-VDAC2 for analyzing its interaction with VP5 in mammalian cells. When lysates of cells expressing both FLAG-VP5 and Myc-VDAC2 were immunoprecipitated with FLAG antibody, Myc-VDAC2 was detected in the precipitate, indicating that VP5 interacted with ectopically expressed VDAC2 in mammalian cells (Fig. 2A). Similar results were obtained in an experiment using the DF-1 cells (Fig. 2B), indicating that the interaction observed between these two proteins is not cell type specific. To confirm that the interaction is in both directions, we transfected HEK293T cells with pCMV-Myc-VDAC2 and/or pRK5-FLAG-VP5 expression plasmids and performed an immunoprecipitation assay with anti-Myc and Western blotting with anti-FLAG monoclonal antibody. The results show that lysates of cells expressing both Myc-VDAC2 and FLAG-VP5 were immunoprecipitated with anti-Myc antibody, FLAG-VP5 was detected in the precipitate (Fig. 2C), indicating that the VP5-VDAC2 interaction is in both directions. To further substantiate the binding of VP5 to VDAC2, we expressed VP5 in HEK293T or DF-1 cells and examined its interaction with endogenous VDAC2 using a pull-down assay. The binding of FLAG-VP5 with endogenous VDAC2 was readily detectable in cells expressing the viral protein (Fig. 2D). These results demonstrate that VP5 interacts with VDAC2 in host cells.

A domain that spans residues 1 to 50 of VP5 is involved in interacting with VDAC2. To determine the region of VP5 responsible for interacting with VDAC2, we constructed a series of VP5 deletion mutants fused to the Myc tag (Fig. 3A). These VP5 derivatives were individually expressed in HEK293T cells, and their ability to interact with VDAC2 was examined by immunoprecipitation. Our results indicated that with the exception of mutants (Δ1 and Δ2) lacking residues 1 to 50, another VP5 mutant including only residues 1 to 50 (Δ4 mutant) retained the ability to interact with VDAC2 (Fig. 3B), indicating that this region of VP5 is important for its interaction with VDAC2 (Fig. 3C).

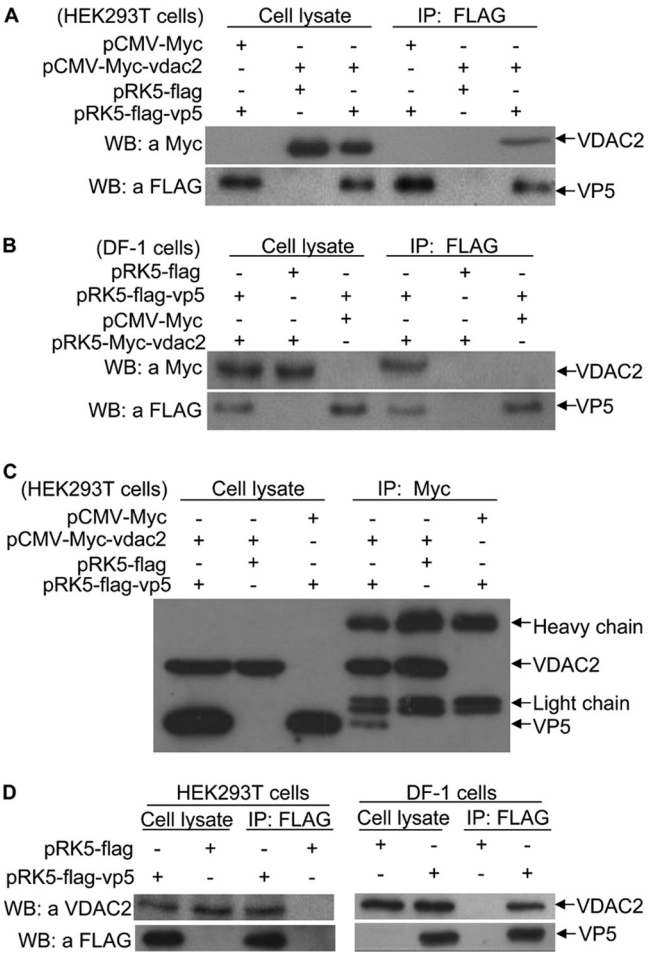

FIG 2 Interaction of VP5 with VDAC2. (A to C) Interaction of IBDV VP5 with exogenous VDAC2. HEK293T cells (A) and DF-1 cells (B) were transfected with the indicated expression plasmids. Twenty-four hours after transfection, cell lysates were prepared and immunoprecipitated (IP) with anti-FLAG antibody and immunoblotted with anti-FLAG or anti-Myc antibodies. (C) Cell lysates were prepared as described above, immunoprecipitated with anti-Myc antibody, and immunoblotted with anti-FLAG or anti-Myc antibodies. (D) Interaction of VP5 with endogenous VDAC2. HEK293T cells or DF-1 cells were transfected with pRK5-FLAG-VP5 or empty vector as a control. Thirty-six hours after transfection, cell lysates were prepared and immunoprecipitated with anti-FLAG antibody and immunoblotted with anti-FLAG or anti-VDAC2 antibodies.

VP5 colocalizes with VDAC2 in the mitochondrion of host cells. To determine the subcellular localization of VP5 and VDAC2, we performed confocal microscopy assay with HEK293T cells transfected to express DsRed-VP5 and GFP-VDAC2. Under this condition, both DsRed-VP5 and GFP-VDAC2 were primarily found in the cytoplasm (Fig. 4A to C). To determine whether endogenous VDAC2 colocalizes to the same cellular compartment, we expressed GFP-VP5 in HEK293T cells by transfection. Transfected samples were immunostained with anti-VDAC2 antibody and a rhodamine (TRITC)-conjugated goat antirabbit antibody. Consistent with the above-described observation, the endogenous VDAC2 was also colocalized with VP5 in the cytoplasm (Fig. 4D to F). To consolidate our findings that VDAC2 colocal-

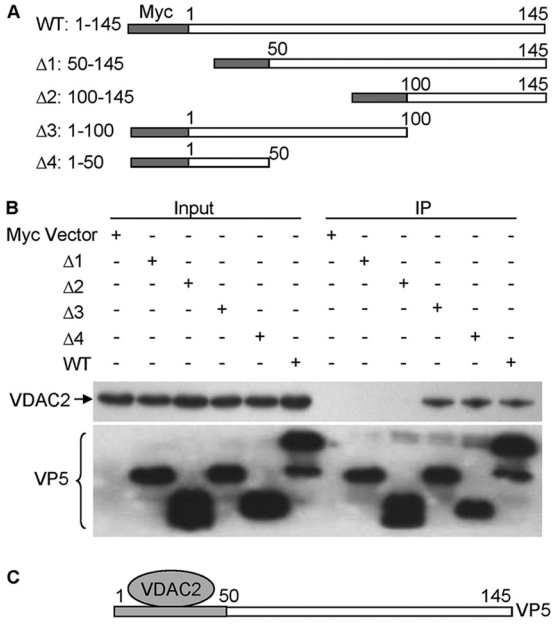

FIG 3 The portion of VP5 from amino acids 1 to 50 is responsible for binding to VDAC2. (A) Schematics represent the genes encoding the full-length VP5 and truncated VP5 molecules (Δ1 through Δ4). The numbers indicate the amino acid positions in the molecule. (B) Endogenous VDAC2 interacted with different truncated VP5 proteins. HEK293T cells (4×10^5) were transfected with full-length Myc-VP5 (wild type [WT]) and different truncated Myc-VP5 molecules (Δ1, aa 50 to 145; Δ2, aa 100 to 145; Δ3, aa 1 to 100; Δ4, aa 1 to 50) or empty vectors. Thirty-six hours after transfection, cell lysates were prepared and immunoprecipitated with anti-Myc monoclonal antibody. The pellets were examined by Western blotting using anti-VDAC2 monoclonal antibody. (C) Schematic representing the binding domain (amino acids 1 to 50) of VP5 for VDAC2.

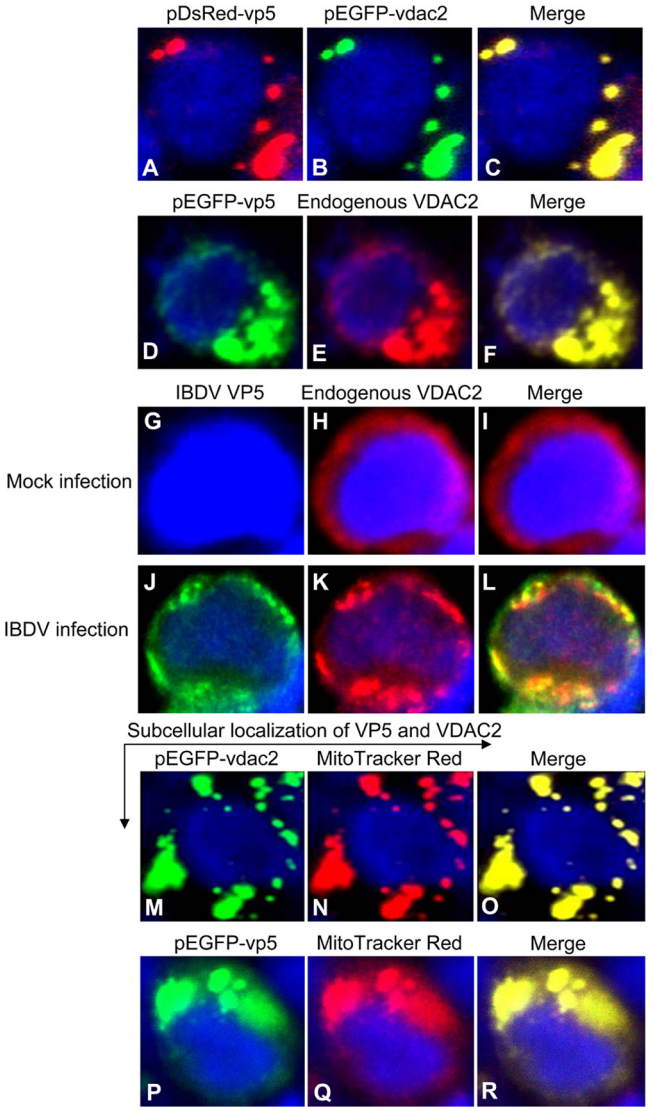

FIG 4 Colocalization of VP5 with VDAC2 in the mitochondrion. (A to C) Localization of exogenous VP5 and VDAC2. HEK293T cells (2×10^5) were seeded on 24-well plates with coverslips in the wells and cultured overnight. Cells were cotransfected with pDsRed-VP5 and pEGFP-VDAC2. Twenty-four hours after transfection, cells were fixed with 1% paraformaldehyde. After washes, the cell nuclei were counterstained with DAPI (blue). The cell samples were observed with a laser confocal scanning microscope. (D to F) Colocalization of VP5 with endogenous VDAC2. HEK293T cells were transfected with pEGFP-VP5 plasmid. Twenty-four hours after transfection, cells were fixed with 1% paraformaldehyde. After washes, the fixed cells were permeabilized with 0.1% Triton X-100 and immunostained with anti-VDAC2 and TRITC-conjugated secondary antibodies. Nuclei were counterstained with DAPI (blue). The cell samples were observed with a laser confocal scanning microscope. (G to L) Colocalization of IBDV VP5 with endogenous VDAC2 in IBDV-infected cells. HEK293T cells were mock infected or infected with IBDV at an MOI of 10. Twenty-four hours after infection, cells were fixed and probed with mouse anti-VP5 antiserum antibody and rabbit anti-VDAC2 antibodies, followed by the FITC-conjugated goat antimouse antibody (green) and TRITC-conjugated goat antirabbit antibody (red). Nuclei were counterstained with DAPI (blue). The cell samples were observed with a laser confocal scanning microscope. (M to R) Colocalization of VP5 with VDAC2 in the mitochondrion. HEK293T cells were transfected with pEGFP-VDAC2 or pEGFP-VP5 plasmids. Twenty-four hours after transfection, cells were stained by MitoTracker Red for the mitochondrion and observed under a laser confocal scanning microscope.

izes with VP5, we examined the interaction of VP5 with VDAC2 in IBDV-infected cells using immunofluorescent-antibody assay (IFA). We infected cells with IBDV at an MOI of 10 and performed IFA using anti-VP5 and anti-VDAC2 antibodies. As expected, endogenous VDAC2 was also colocalized with VP5 in IBDV-infected cells (Fig. 4G to L). In addition, transfection of HEK293T cells with pEGFP-VDAC2 or pEGFP-VP5 indicated that both VDAC2 and VP5 were located in mitochondria (Fig. 4M to R). These results clearly demonstrate that VP5 interacts with VDAC2 and they are both located in the mitochondrion.

VDAC2 inhibitor DIDS inhibits VP5- or IBDV-induced apoptosis and restricts viral release. The binding of VP5 to VDAC2 suggests that VDAC2 plays an important role in VP5-induced apoptosis. Thus, inhibition of VDAC2 function is predicted to interfere with VP5-induced apoptosis. To test this hypothesis, we first examined the effects of the VDAC inhibitor DIDS on VP5-induced apoptosis in DF-1 cells. The addition of DIDS to cells expressing GFP-VP5 completely abolished the cell death phenotype (Fig. 5A and B). To rule out the possibility that apoptosis induced by VP5 overexpression was a result of secondary effects derived from VP5 protein overaccumulation, we infected DF-1 cells with the IBDV *Lx* strain in the presence of DIDS. Consistent with the results observed in transfection experiments, DIDS abolished apoptosis induced by IBDV infection (Fig. 5C and D). In addition, we examined the effect of DIDS on virus replication and found that the viral loads in the cell culture treated with

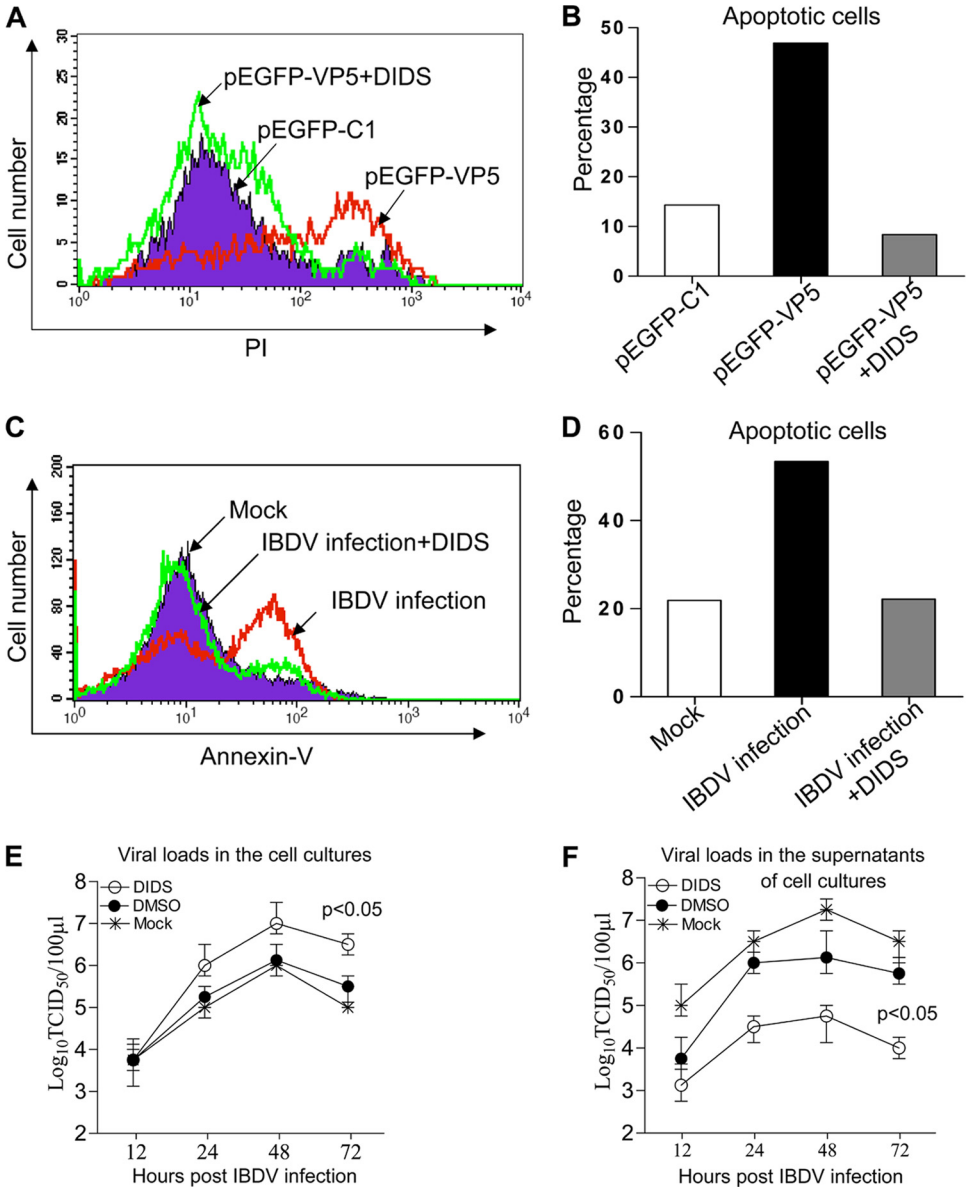

FIG 5 Inhibited VP5- or IBDV-induced apoptosis and restricted viral release in DF-1 cells treated by the VDAC inhibitor DIDS. (A) Inhibition of IBDV VP5-induced apoptosis in DF-1 cells by DIDS. DF-1 cells (6×10^5) were seeded on six-well plates and cultured overnight. Cells were transfected with pEGFP-C1 or pEGFP-VP5 plasmids by Lipofectamine LTX. Six hours after transfection, cells were cultured in the presence of 10 μM DIDS in dimethyl sulfoxide (DMSO; final concentration, <1% [vol/vol]) for 3 h. Three hours after incubation, medium was changed with fresh DMEM. Twenty-four hours after transfection, cells were harvested and stained with PI, followed by flow cytometry analysis. GFP-positive cells were gated for the further analysis of PI staining-positive cells. (B) Percentage of apoptotic cells transfected with pEGFP-C1 or pEGFP-VP5 with or without 10 μM DIDS. (C) Inhibition of IBDV-induced apoptosis in DF-1 cells by DIDS. DF-1 cells (6×10^5) were seeded on six-well plates and cultured overnight. Cells were mock infected or infected with IBDV at an MOI of 10 at 37°C for 3 h and then washed with PBS before incubation with DIDS (100 μM) or dimethyl sulfoxide for 3 h. Cells were again washed with PBS, followed by incubation with 10% DMEM. Thirty-six hours postinfection, cells were harvested and stained with annexin V-FITC and analyzed by flow cytometry. (D) Percentage of apoptotic cells after mock or IBDV infection in the presence of DIDS or dimethyl sulfoxide as a control. Data are representative of three independent experiments. (E and F) Effects of DIDS on IBDV growth and viral release. DF-1 cells were infected with IBDV (MOI = 10). Three hours after infection, cells were washed with PBS and then incubated with 100 μM DIDS or dimethyl sulfoxide for another 3 h. Cells were again washed with PBS, followed by incubation with 10% DMEM. At different time points (12, 24, 48, and 72 h) after IBDV infection, the viral loads in the cell cultures (E) and the supernatants (F) were determined by $TCID_{50}$ determination using 96-well plates. The significance of the difference between DIDS-treated cells and controls was performed by ANOVA ($P < 0.05$). The graph shows the average of the viral loads in DF-1 cells from three individual experiments.

DIDS were greater than those of the control ($P < 0.05$) (Fig. 5E). In contrast, the viral loads in the supernatants of IBDV-infected cells markedly decreased after DIDS treatment compared to those of the control ($P < 0.05$) (Fig. 5F). These results suggest that the enhanced IBDV growth and restricted viral release might be associated with the inhibition of IBDV-induced apoptosis by DIDS. Together, these results indicate that VP5-induced apoptosis is mediated by VDAC.

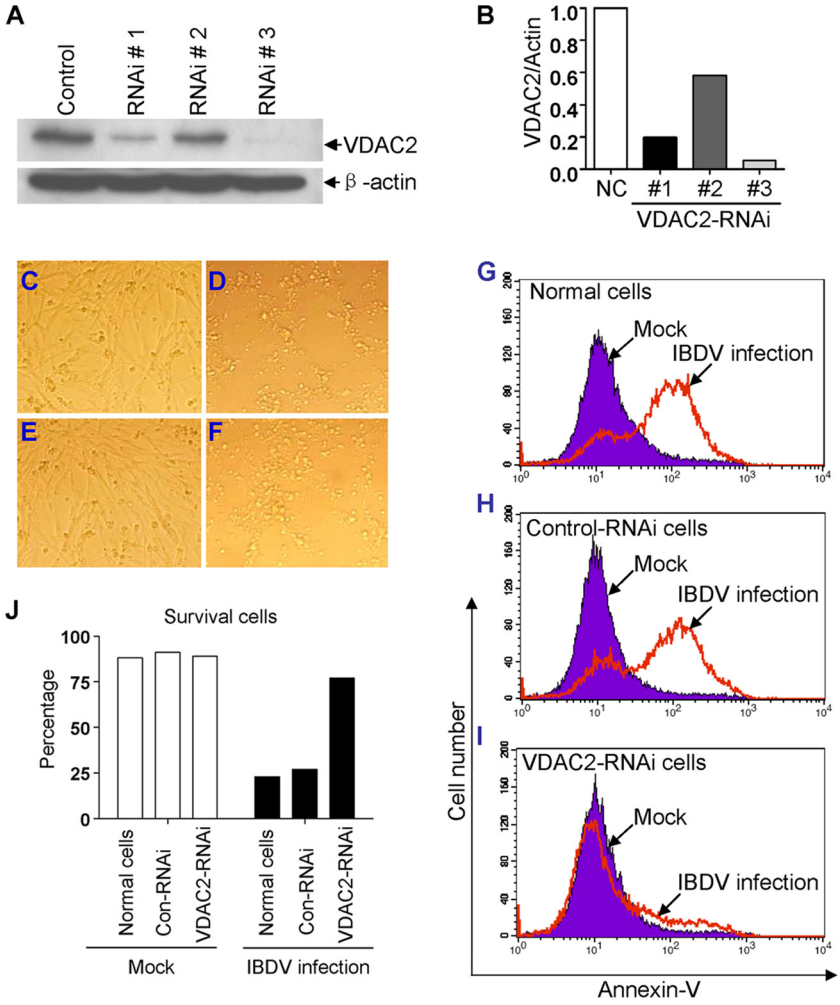

FIG 6 Knockdown of VDAC2 inhibits IBDV-induced apoptosis. (A) Effects of VDAC2 RNAi on the expression of endogenous VDAC2. DF-1 cells (4×10^5) were transfected with siRNA (RNAi#1 to RNAi#3) or controls as described in Materials and Methods. Forty-eight hours after the second transfection, cell lysates were prepared and examined by Western blotting with anti-VDAC2 antibody. Endogenous β-actin expression was used as an internal control. (B) Relative levels of VDAC2 in VDAC2 RNAi-treated cells. The density of bands in panel A was quantitated by densitometry. The relative levels of VDAC2 were calculated as follows: band density of VDAC2/band density of β-actin. NC, nontreated control. (C to F) Representative morphological changes of DF-1 cells after infection with IBDV or mock infection. VDAC2 RNAi cells (E), control RNAi cells (F), and normal DF-1 cells (D) were infected with IBDV at an MOI of 10. Thirty-six hours after infection with IBDV, cells were examined by phase-contrast microscopy. Mock-infected normal DF-1 cells were used as a control (C). Magnification, ×200. (G to I) Knockdown of VDAC2 inhibited IBDV-induced apoptosis. Normal DF-1 cells (G), control RNAi cells (H), and VDAC2 RNAi cells (I) were mock infected or infected with IBDV at an MOI of 10. Thirty-six hours postinfection, cells were harvested and stained with annexin V-FITC and PI, followed by flow cytometry analysis. (J) Percentage of surviving DF-1 cells, control (Con) RNAi cells, and VDAC2 RNAi cells with mock or IBDV infection. Data are representative of three independent experiments.

Knockdown of VDAC2 inhibits IBDV-induced apoptosis. The facts that the VP5 protein is mainly responsible for IBDV-induced apoptosis and the inhibition of VDAC2 activity led to abolishment of VP5-induced apoptosis suggest that VDAC2 might play a critical role in IBDV-induced apoptosis and that knockdown of VDAC2 would therefore affect IBDV-induced apoptosis. To test this hypothesis, we made three VDAC2 RNAi constructs and found that one can effectively lower the cellular level of VDAC2 without causing discernible changes in cell morphology (Fig. 6A and B). We then infected DF-1 cells receiving this siRNA or control siRNA with the IBDV *Lx* strain. As a result, knockdown of VDAC2 markedly reduced the IBDV-induced CPE (Fig. 6C to F). Similarly, when examined by flow cytometry using annexin V and PI staining, cells receiving the siRNA against VDAC2 displayed significantly lower levels of IBDV-induced apoptosis (Fig. 6G to I), and this was accompanied by higher rates of survival among IBDV-infected cells (Fig. 6J). These data strongly suggest that VDAC2 plays a critical role in IBDV-induced apoptosis in DF-1 cells.

VDAC2 is required for the activation of caspase-9 and -3 and release of cytochrome *c* during IBDV infection. Because VDAC2 localizes to the mitochondrion, it may potentiate the activation of caspase-9 and caspase-3 seen during IBDV infection. In addition, previous studies indicated that VDAC2 is critical for the release of cytochrome *c* from mitochondria to the cytoplasm (15, 27). Thus, we examined the activities of these two caspases and the cytochrome *c* release in siRNA-treated, IBDV-infected DF-1 cells. In samples receiving the control siRNA, the activities of caspase-9

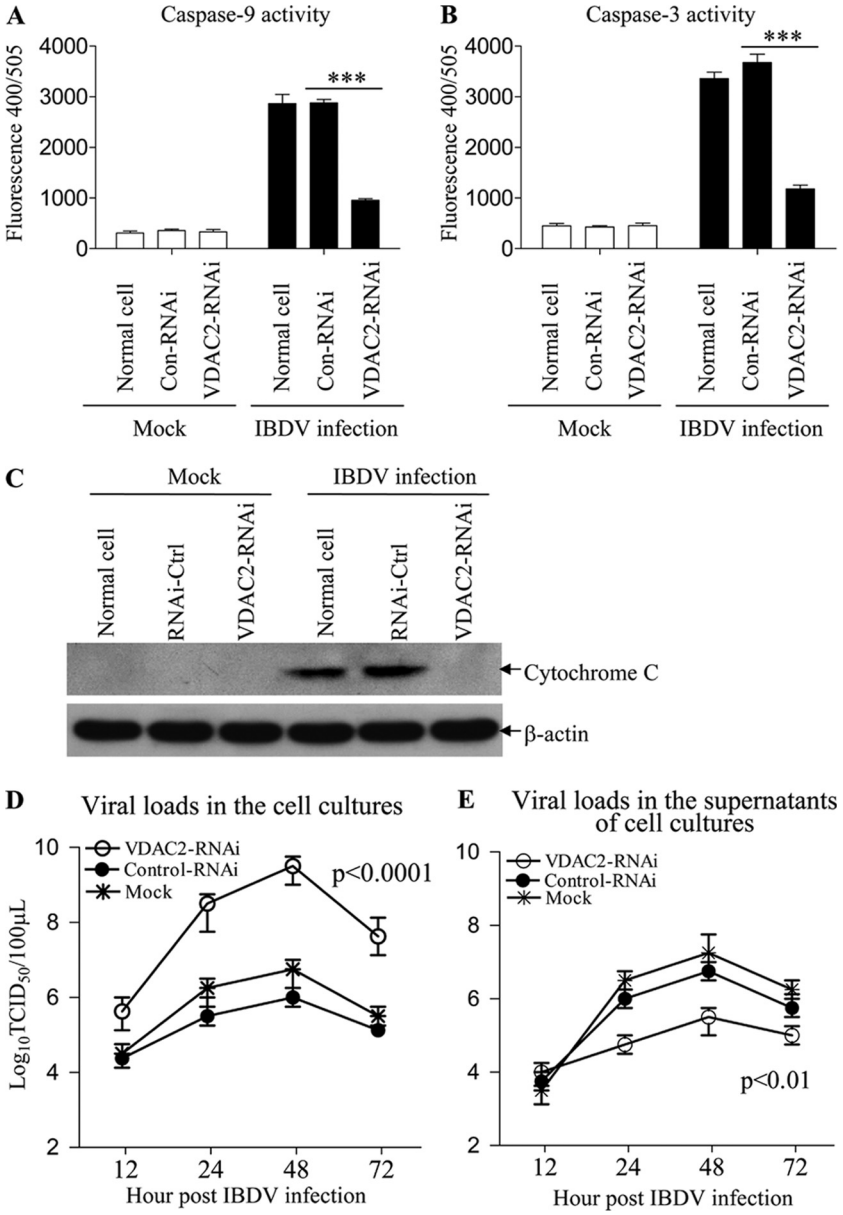

FIG 7 Knockdown of VDAC2 inhibited IBDV-induced activation of caspase-9 and -3 and release of cytochrome *c* and enhanced IBDV growth. (A and B) Normal DF-1 cells, control RNAi cells, and VDAC2 RNAi cells were mock infected or infected with IBDV at an MOI of 10. Twenty hours postinfection, the enzymatic activities of caspase-9 and -3 were examined as described in Materials and Methods. (C) Western blot analysis of cytochrome *c* (14 kDa) and β-actin (42 kDa) in cytosolic fractions prepared from normal DF-1 cells, RNAi control cells, and VDAC2 RNAi cells mock infected or infected with IBDV at an MOI of 10 for 24 h. Data are representative of three independent experiments. (D and E) Mock-transfected cells, control RNAi cells, and VDAC2 RNAi cells were infected with IBDV at an MOI of 10. At different time points (12, 24, 48, and 72 h) after IBDV infection, the viral titers in the cell cultures (D) or supernatants (E) were determined by $TCID_{50}$ analysis using 96-well plates. The significance of the difference between VDAC2 RNAi and control RNAi treatments was performed by ANOVA ($P < 0.001$). The graph shows the average of viral titers in DF-1 cells from three individual experiments.

and caspase-3 as well as the release of cytochrome *c* were markedly enhanced upon IBDV infection (Fig. 7A to C). In contrast, similar infection did not lead to such increases in cells treated with VDAC2-specific siRNA. These results clearly demonstrate that VDAC2 is involved in the activation of caspase-9 and -3 and the release of cytochrome *c* during IBDV infection.

Knockdown of VDAC2 enhances IBDV growth but restricts IBDV release from host cells. Apoptosis is a defense mechanism of host cells in response to virus infection to limit viral propagation. The fact that VDAC2 mediates IBDV-induced apoptosis prompted us to determine the role of VDAC2 in the replication of IBDV. We then knocked down VDAC2 in DF-1 cells with siRNA and examined the viral replication in these cells by measuring viral loads in the culture of IBDV-infected cells at different time points postinfection. Consistent with its postulated role in restricting IBDV growth, cells with lower VDAC2 levels support more robust IBDV growth (Fig. 7D); however, the viral titers in the supernatants of VDAC2-knocked-down cell cultures were significantly

lower than those in the supernatants of control RNAi cell cultures ($P < 0.01$) (Fig. 7E), indicating that viral particle release from these cells is restricted. These results suggest that VDAC2-mediated apoptosis is an important strategy employed by host cells to limit viral propagation but might also be taken advantage of by the virus to spread.

DISCUSSION

IBD is an acute, highly contagious viral disease causing damage in lymphoid organs in birds, especially the bursa of Fabricius (20). Importantly, the surviving IBDV-infected chickens suffer from immunosuppression with compromised humoral and cellular immune responses (28, 34), leading to susceptibility of the chickens to other diseases. To some extent, IBDV for birds is akin to HIV for humans. Thus, IBD remains a threat to the poultry industry worldwide.

Although IBDV-induced apoptosis in host cells has been very well established (6, 11, 13, 25, 32, 35) and VP5 was held responsible (40, 41), the exact molecular mechanisms for such induction are unclear. IBDV infection causes apoptosis in multiple chicken cells, including peripheral blood lymphocytes (35), B cells (25), and CEF and DF-1 cells (32, 37). Consistent with these observations (32, 37), we found that IBDV infection caused extensive apoptosis in DF-1 cells. We thus used DF-1 cells as a model to investigate the molecular mechanisms underlying IBDV-induced apoptosis. On the basis of the hypothesis that the IBDV-induced apoptosis was triggered by interaction of one or more viral proteins with the host molecules involved in apoptotic signaling, we screened the viral proteins (VP2 to VP5) for their ability to induce apoptosis in DF-1 cells. However, VP1 was not screened because it is known to be a putative RNA-dependent RNA polymerase (RdRp) (19, 36). We found that both VP2 and VP5 caused apoptosis in DF-1 cells. This result was consistent with earlier observations that these two proteins cause cell death in the chicken B-cell line RP9 and CEFs (41). In addition, our data showed that the rate of apoptotic cells caused by VP5 was at least threefold higher than that caused by VP2. Apparently, VP5 was more potent than VP2 in the induction of apoptosis in DF-1 cells, even though VP2 was first recognized to be an apoptosis inducer (6).

VP5 of IBDV is a nonstructural protein and not essential for viral replication (21). It was found that accumulation of VP5 within the host plasma membrane induced cell lysis (18). In the present study, we first determined that VP5 is mainly responsible for IBDV-induced apoptosis in DF-1 cells, as examined by flow cytometry using annexin V and PI staining. Second, VP5 specifically interacts with VDAC2 under all tested conditions. We can readily detect the binding between VP5 and endogenous VDAC2 (Fig. 2D, Fig. 4D to F and J to L). Third, the abolishment of apoptosis induced by VP5 expression or IBDV infection can be achieved by the inhibition of VDAC2 activity or knockdown of VDAC2 expression (Fig. 5 and 6). Finally, VDAC2-mediated apoptosis restricts viral growth but may also be required for the viral particle release (Fig. 7D and E). To further investigate the effect of VDAC2 knockdown on IBDV growth and spread between cells, we infected VDAC2 RNAi cells or RNAi controls with IBDV at an MOI of 0.5. Consistently, we also found that knockdown of VDAC2 by siRNA enhanced viral loads in the cultures, while the viral titers in the supernatants decreased compared to that of the RNAi control. Clearly, the reduced level of cell death in VDAC2-knockdown cells during viral replication was not a result of less efficiency in viral uptake because these cells support better viral replication.

VDAC2 is one of the isoforms of VDACs capable of pore formation in the outer mitochondrial membrane and involved in apoptosis (3, 4, 29, 42). It was reported that VDAC2 is a mitochondrial outer membrane protein associated with the proapoptotic effector BAK, which initiates the mitochondrial phase of apoptosis (4). A second proapoptotic protein, Bid, was also reported to regulate the VDAC channel (26). Our data and those from previous studies indicated that IBDV-induced apoptosis or VDAC-mediated apoptosis is associated with cytochrome *c* release (15, 27). However, VDAC2 knockdown inhibited the activities of caspase-9 and -3 and the release of cytochrome *c* during IBDV-induced apoptosis, suggesting that IBDV-induced apoptosis follows the intrinsic apoptotic pathway. As such, these observations raised several questions. For example, what kind of signaling event is triggered by VDAC2 upon interaction with VP5? Does VDAC2 directly initiate the cell death signaling event or is the initiation achieved by the action of BAK or Bid? Similarly, what molecular feature of VP5 that interacts with VDAC2 leads to cell death? Finally, is VP5-induced apoptosis critical to viral spread? We prefer a model in which VDAC2 functions to sense the presence of the virus and triggers cell death to limit viral proliferation. This model is consistent with the fact that apoptosis, or programmed cell death, is a controlled physiological process of the host to eliminate unwanted cells, including those infected by virus. Thus, apoptosis is a defense mechanism in response to viral infection. In light of these observations, it is not surprising that some viruses carry antiapoptotic factors to inhibit apoptosis at the early stage of viral infection (17). On the other hand, for some viruses, triggering apoptosis at the late stage of viral replication is important for the release of viral particles after cellular nutrients have been depleted (7, 8). Clearly, viruses have evolved distinct mechanisms to exploit host apoptotic processes for their own benefit.

Liu and Vakharia proposed that VP5 might play a role as an antiapoptotic protein in an early stage of infection (17). Recently, an article reported that VP5 may act as an antiapoptotic molecule by binding to the p85alpha subunit of PI3K early during IBDV infection (38). These results suggest that VP5-induced antiapoptosis is an important event to support viral replication in the early stage of IBDV infection. Our data show that VP5 induces apoptosis by binding to VDAC2 in the later stage of IBDV infection to facilitate viral release because viral release was inhibited in cells with a reduced level of VDAC or DIDS treatment. In addition, Qin and colleagues reported that VP5-deficient mutant IBDV caused reductions in bursal lesions of specific-pathogen-free chickens compared to the parental virus, indicating that VP5 induces tissue damage (23). These results suggest that VP5 is a crucial viral component exploited by IBDV for inhibiting cellular apoptosis early during IBDV infection to gain sufficient time for its replication but inducing apoptosis in host cells at later stages of IBDV infection to facilitate its release.

We propose that IBDV VP5 may play different roles at different stages of viral infection, depending on the binding affinity of target proteins with VP5 and the quantity of VP5 in the cytoplasm. In this case, mathematic biology may be required to decipher the multiple functions of VP5.

In the present study, we found that inhibition of IBDV-induced apoptosis by VDAC2 knockdown enhanced viral growth but restricted viral release, as demonstrated by an increased viral

load in the culture of cells with VDAC2 knockdown and a decreased viral titer in the supernatants of these cultures (Fig. 7D and E). However, on the basis of the result that monoclonal VP5-expressing Vero cells did not exhibit induction of cell death, it was suggested that the VP5 protein of IBDV promotes virion release from infected cells and is not involved in cell death (39). This discrepancy may result from the possibility that Vero cells are not the natural host of IBDV. Therefore, Vero cells may not be an ideal cell model to investigate the mechanism underlying IBDV-induced apoptosis.

In summary, our results revealed that IBDV VP5, a major apoptosis inducer in host cells, interacts with voltage-dependent anion channel 2 (VDAC2) to trigger host cell death during IBDV infection. The observation that knockdown of VDAC2 markedly inhibited IBDV-induced apoptosis and enhanced viral growth in host cells but restricted the release of viral particles suggests that VDAC2 plays a critical role in IBDV-induced apoptosis and control of viral growth. These findings have provided insights for further studies of the molecular mechanism of IBDV infection.

ACKNOWLEDGMENTS

We thank Jun Tang for her technical assistance and Zhao-Qing Luo for comments and discussions.

This work was supported by grants from the National Natural Science Foundation of China (grants 30725026 and 31072117), Earmarked Fund for Modern Agro-Industry Technology Research System (grant NYCYTX-41), and the Program for Cheung Kong Scholars and Innovative Research Team in University of China (grant NO.IRT0866).

REFERENCES

1. **Azad AA, Barrett SA, Fahey KJ.** 1985. The characterization and molecular cloning of the double-stranded RNA genome of an Australian strain of infectious bursal disease virus. Virology **143**:35–44.
2. **Birghan C, Mundt E, Gorbalenya AE.** 2000. A non-canonical lon proteinase lacking the ATPase domain employs the Ser-Lys catalytic dyad to exercise broad control over the life cycle of a double-stranded RNA virus. EMBO J. **19**:114–123.
3. **Cesar MC, Wilson JE.** 2004. All three isoforms of the voltage-dependent anion channel (VDAC1, VDAC2, and VDAC3) are present in mitochondria from bovine, rabbit, and rat brain. Arch. Biochem. Biophys. **422**: 191–196.
4. **Cheng EH, Sheiko TV, Fisher JK, Craigen WJ, Korsmeyer SJ.** 2003. VDAC2 inhibits BAK activation and mitochondrial apoptosis. Science **301**:513–517.
5. **Dobos P, et al.** 1979. Biophysical and biochemical characterization of five animal viruses with bisegmented double-stranded RNA genomes. J. Virol. **32**:593–605.
6. **Fernandez-Arias A, Martinez S, Rodriguez JF.** 1997. The major antigenic protein of infectious bursal disease virus, VP2, is an apoptotic inducer. J. Virol. **71**:8014–8018.
7. **Galluzzi L, Brenner C, Morselli E, Touat Z, Kroemer G.** 2008. Viral control of mitochondrial apoptosis. PLoS Pathog. 4:e1000018.
8. **Hay S, Kannourakis G.** 2002. A time to kill: viral manipulation of the cell death program. J. Gen. Virol. **83**:1547–1564.
9. **Hudson PJ, McKern NM, Power BE, Azad AA.** 1986. Genomic structure of the large RNA segment of infectious bursal disease virus. Nucleic Acids Res. **14**:5001–5012.
10. **Jagadish MN, Staton VJ, Hudson PJ, Azad AA.** 1988. Birnavirus precursor polyprotein is processed in Escherichia coli by its own virus-encoded polypeptide. J. Virol. **62**:1084–1087.
11. **Jungmann A, Nieper H, Muller H.** 2001. Apoptosis is induced by infectious bursal disease virus replication in productively infected cells as well as in antigen-negative cells in their vicinity. J. Gen. Virol. **82**: 1107–1115.
12. **Kibenge FS, McKenna PK, Dybing JK.** 1991. Genome cloning and analysis of the large RNA segment (segment A) of a naturally avirulent serotype 2 infectious bursal disease virus. Virology **184**:437–440.
13. **Kong LL, Omar AR, Hair-Bejo M, Aini I, Seow HF.** 2004. Comparative analysis of viral RNA and apoptotic cells in bursae following infection with infectious bursal disease virus. Comp. Immunol. Microbiol. Infect. Dis. **27**:433–443.
14. **Lejal N, Da CB, Huet JC, Delmas B.** 2000. Role of Ser-652 and Lys-692 in the protease activity of infectious bursal disease virus VP4 and identification of its substrate cleavage sites. J. Gen. Virol. **81**:983–992.
15. **Liu J, Wei L, Jiang T, Shi L, Wang J.** 2007. Reduction of infectious bursal disease virus replication in cultured cells by proteasome inhibitors. Virus Genes **35**:719–727.
16. **Liu M, Vakharia VN.** 2004. VP1 protein of infectious bursal disease virus modulates the virulence in vivo. Virology **330**:62–73.
17. **Liu M, Vakharia VN.** 2006. Nonstructural protein of infectious bursal disease virus inhibits apoptosis at the early stage of virus infection. J. Virol. **80**:3369–3377.
18. **Lombardo E, Maraver A, Espinosa I, Fernandez-Arias A, Rodriguez JF.** 2000. VP5, the nonstructural polypeptide of infectious bursal disease virus, accumulates within the host plasma membrane and induces cell lysis. Virology **277**:345–357.
19. **Macreadie IG, Azad AA.** 1993. Expression and RNA dependent RNA polymerase activity of birnavirus VP1 protein in bacteria and yeast. Biochem. Mol. Biol. Int. **30**:1169–1178.
20. **Muller H, Islam MR, Raue R.** 2003. Research on infectious bursal disease—the past, the present and the future. Vet. Microbiol. **97**:153–165.
21. **Mundt E, Kollner B, Kretzschmar D.** 1997. VP5 of infectious bursal disease virus is not essential for viral replication in cell culture. J. Virol. **71**:5647–5651.
22. **Pitcovski J, et al.** 2003. Development and large-scale use of recombinant VP2 vaccine for the prevention of infectious bursal disease of chickens. Vaccine **21**:4736–4743.
23. **Qin L, et al.** 2010. VP5-deficient mutant virus induced protection against challenge with very virulent infectious bursal disease virus of chickens. Vaccine **28**:3735–3740.
24. **Reed LJ, Muench H.** 1938. A simple method of estimating fifty percent endpoints. Am. J. Epidemiol. **27**:493–497.
25. **Rodriguez-Lecompte JC, Nino-Fong R, Lopez A, Frederick Markham RJ, Kibenge FS.** 2005. Infectious bursal disease virus (IBDV) induces apoptosis in chicken B cells. Comp. Immunol. Microbiol. Infect. Dis. **28**:321–337.
26. **Rostovtseva TK, et al.** 2004. Bid, but not Bax, regulates VDAC channels. J. Biol. Chem. **279**:13575–13583.
27. **Roy SS, Ehrlich AM, Craigen WJ, Hajnoczky G.** 2009. VDAC2 is required for truncated BID-induced mitochondrial apoptosis by recruiting BAK to the mitochondria. EMBO Rep. **10**:1341–1347.
28. **Sharma JM, Kim IJ, Rautenschlein S, Yeh HY.** 2000. Infectious bursal disease virus of chickens: pathogenesis and immunosuppression. Dev. Comp. Immunol. **24**:223–235.
29. **Shoshan-Barmatz V, et al.** 2010. VDAC, a multi-functional mitochondrial protein regulating cell life and death. Mol. Aspects Med. **31**:227–285.
30. **Spies U, Muller H, Becht H.** 1989. Nucleotide sequence of infectious bursal disease virus genome segment A delineates two major open reading frames. Nucleic Acids Res. **17**:7982.
31. **Stricker RL, Behrens SE, Mundt E.** 2010. Nuclear factor NF45 interacts with viral proteins of infectious bursal disease virus and inhibits viral replication. J. Virol. **84**:10592–10605.
32. **Tham KM, Moon CD.** 1996. Apoptosis in cell cultures induced by infectious bursal disease virus following in vitro infection. Avian Dis. **40**: 109–113.
33. **Upadhyay C, Ammayappan A, Patel D, Kovesdi I, Vakharia VN.** 2011. Recombinant infectious bursal disease virus carrying hepatitis C virus epitopes. J. Virol. **85**:1408–1414.
34. **van den Berg TP, Eterradossi N, Toquin D, Meulemans G.** 2000. Infectious bursal disease (Gumboro disease). Rev. Sci. Tech. **19**:509–543.
35. **Vasconcelos AC, Lam KM.** 1994. Apoptosis induced by infectious bursal disease virus. J. Gen. Virol. **75**(Pt 7):1803–1806.
36. **von Einem UI, et al.** 2004. VP1 of infectious bursal disease virus is an RNA-dependent RNA polymerase. J. Gen. Virol. **85**:2221–2229.
37. **Wang Y, et al.** 2009. Comparative study of the replication of infectious bursal disease virus in DF-1 cell line and chicken embryo fibroblasts evaluated by a new real-time RT-PCR. J. Virol. Methods **157**:205–210.
38. **Wei L, et al.** 2011. Infectious bursal disease virus activates the phosphatidylinositol 3-kinase (PI3K)/Akt signaling pathway by interaction of VP5 protein with the p85alpha subunit of PI3K. Virology **417**: 211–220.

39. **Wu Y, Hong L, Ye J, Huang Z, Zhou J.** 2009. The VP5 protein of infectious bursal disease virus promotes virion release from infected cells and is not involved in cell death. Arch. Virol. **154**:1873–1882.
40. **Yao K, Goodwin MA, Vakharia VN.** 1998. Generation of a mutant infectious bursal disease virus that does not cause bursal lesions. J. Virol. **72**:2647–2654.
41. **Yao K, Vakharia VN.** 2001. Induction of apoptosis in vitro by the 17-kDa nonstructural protein of infectious bursal disease virus: possible role in viral pathogenesis. Virology **285**:50–58.
42. **Yuqi L, et al.** 2009. Voltage-dependent anion channel (VDAC) is involved in apoptosis of cell lines carrying the mitochondrial DNA mutation. BMC Med. Genet. **10**:114.